Vol. 18(4), pp. 106-115, October-December, 2023
DOI: 10.5897/IJPS2023.5048
Article Number: A2C289B71503
ISSN: 1992-1950

http://www.academicjournals.org/IJPS

ACADEMIC JOURNALS
expand your knowledge

International Journal of Physical Sciences

Full Length Research Paper

foF2 diurnal variation at Dakar station during the period of geomagnetic shock of variable duration over solar cycle 21 and 22: Prediction with IRI 2016

Ali Mahamat Nour[1]*, Douzane Gouara[2], Sibri Alphonse Sandwidi[3] and Frédéric Ouattara[3]

[1]Department of Physics, Faculty of Exact and Applied Sciences, University of N'Djamena, N'Djamena, Chad.
[2]Laboratory of Physics of the Atmosphere, Climate and Environment (LaPACE), University of Negauena, Chad.
[3]Laboratory of Applied Chemistry and Space and Energy Physics (LACAPSE), University of Koudougou, Burkina Faso.

Received 11 September, 2023; Accepted 1 November, 2023

This work concerns the comparative study of the diurnal variation of the critical frequency of the F2 layer (foF2) between experimental data from the Dakar station and those of the IRI 2016 model through its URSI. The comparison was conducted during solar cycles 21 and 22, across different phases, and on various days of geomagnetic shock activity. The results indicate that during solar minimum, the graphs of the experimental data generally exhibit the signature of vertical drift, whereas the IRI model presents a plateau profile indicative of the absence of an electrojet. During this phase, the highest deviation percentages were typically observed around sunrise. The results also demonstrate that at the Dakar station, the increasing phase was characterized by a pre-reversal of the electric field on different shock days. Regardless of the duration of the shock, the decreasing phase was marked by the complete absence of an electrojet, as observed in both sets of data. The quantitative study reveals that at solar maximum, our results exhibit a strong correlation between the experimental data and the IRI model. Throughout all phases, predictions were accurate during the daytime and exhibited high values around sunrise.

Key words: foF2, geomagnetic shock activity, IRI model 2016 prediction, solar cycle, sub-programme URSI.

INTRODUCTION

Since the discovery of the ionosphere by Marconi in 1901 during a transatlantic radio link, research into this upper part of the atmosphere has intensified worldwide, and it continues to contribute significantly to the understanding of ionospheric variability. Through its F2 layer, the ionosphere plays a crucial role in the propagation of radio waves in specific frequency ranges, both for terrestrial communications and earth-satellite links. Recognizing its utility, supprimer have been developed, validated, and approved using in situ measurement data. It was with this recognition in mind that the IRI (International Reference Ionospheric) model was created. The IRI model is a

*Corresponding author. E-mail: nouralimht@yahoo.fr.

virtual observatory known as the virtual ionosphere, thermosphere, mesosphere, Observatory, developed by a research group jointly supported by the Committee on Space Research (COSPAR) and the International Union of Radio Science (URSI) since 1960. The site includes a database containing readings from the global network of ionosondes and is regularly updated. The IRI employs two sub-programs, URSI and CCIR (Comité Consultatif International des Radio Communications).

A number of studies have been carried out worldwide comparing experimental and IRI data (Adeniyi et al., 2005; Adewale et al., 2010; Batista et al., 1996; Batista and Abdu, 2004; Bertoni et al., 2006; Bittencourt and Chryssafidis, 1994; Chakraborty et al., 2014; Erdinc et al., 2021; Kumar et al., 2014; Liu et al., 2010; Nanéma and Ouattara, 2013; Nanema et al., 2018; Ouattara and Nanéma, 2014; Oyeyemi et al., 2005; Sawadogo et al., 2019; Shastri et al., 1996; Sethi et al., 2007; Zhang et al., 2010).

At the Ouagadougou station, during geomagnetically quiet periods, the 2007 version of the IRI model does not produce a vertical drift signature. However, the 2012 version of the IRI model does reproduce an inverse profile but does not display the first peak of the "noon bite-out" profile. The IRI 2012 version also provides poor predictions during nighttime (Ouattara, 2013; Ouattara and Nanema, 2014). However, during geomagnetic shock periods, the 2012 version of the IRI model reproduces the electrodynamic phenomenon (vertical drift EXB) during the daytime (Segda et al., 2019). A quantitative study based on deviation percentages indicates a good correlation between the URSI sub-programme forecasts and ionosonde data, except during the increasing phase. On the other hand, an investigation using the relative deviation module means shows poor agreement between measured data and IRI forecasts (Sawadogo et al., 2019).

At the Ouagadougou station, the work conducted by Adeniyi et al. (2005) during the years 1985, 1990 and 1993, which correspond to low, high and moderate solar activity years respectively, showed that the IRI representation was very accurate during low and moderate solar activity for both day and night. Nighttime forecasts were particularly accurate when URSI coefficients were used for forecasting.

The diurnal variation of foF2 studied at the Korhogo station from 1992 to 2001 by Guibula et al. (2019) during various geomagnetic activities reveals that during quiet and fluctuating periods, the URSI sub-program of IRI 2012 accurately captures the vertical drift signature during both the increasing and decreasing phases. The quantitative analysis also indicates that the IRI model provides a good agreement with the measured values during daytime across all geomagnetic periods.

Studies conducted on the critical frequency of the F2 layer at the Dakar station during periods of Quiet achinty geomagnetic demonstrate that the predictions were more accurate during the daytime compared to nighttime. Predictions were also more reliable during the increasing phase but less so during other phases where the ExB signature was absent, despite being present in the measured values (Sandwidi et al., 2020). Bittencourt and Chryssafidis (1994) and Batista et al. (1996), using the Fortaleza station in Brazil (4°S, 38°W) and the Cachoeira Paulista station (22.5°S, 45°W), respectively, compared hmF2 (the height of the maximum electron density of the F2 layer) and foF2 observed with the IRI-90 model during different periods of solar activity. Their work demonstrated that the predictions of the IRI-90 model were reasonably accurate for the various solar activities considered, except during the moments following sunset during high solar activity when the IRI-90 notably underestimated the observed hmF2.

Shastri et al. (1996) conducted an analysis comparing observed foF2 data from ionosonde measurements for three low-latitude Indian stations: Delhi (28.6°N, 77.2°E), Ahmedabad (23.0°N, 72.6°E), and Kodaikanal (10.2°N, 77.5°E). Their study also found that the IRI-90 model predictions were reasonably accurate for the different solar activities considered. In research on IRI-2001 model forecasts using ionospheric data from Brazilian low-latitude stations Palmas (10.17°S, 48.20°W) and São José dos Campos (23.20°S, 45.86°W), Bertoni et al. (2006) showed reasonable agreement for both parameters (hmF2 and foF2). However, they noted that some improvements are still necessary to obtain better predictions for equatorial ionospheric regions.

In their comparative study at the Brazilian equatorial station of Sao Luis (2.6°S, 44.2°W, dip - 0.5°) between ionospheric parameters observed and modeled by IRI, Batista and Abdu (2004) emphasized that during a period of high solar activity, there is good agreement between the IRI forecasts and the average foF2 values observed during the day. Adewale et al. (2010), in their work on the monthly averages of ionospheric parameters foF2 and hmF2 during calm and disturbed periods at three South African stations: Grahamstown, 33.3°S, 26°E; Madimbo, 22.4°S, 26°E; and Louisvale, 28.5°S, 21°E, using IRI 2001 (CCIR and URSI), have shown that IRI-2001 predicts agreement with observed ionosonde data to varying degrees depending on the location.

On average, the model correctly describes daily and seasonal variations in foF2 and hmF2. Nevertheless, some anomalies between predictions and observations have been identified. Oyeyemi et al. (2005) also compared observed values of foF2 with predictions from both a neural network and the IRI model. Their results emphasize the necessity to improve the IRI model for more accurate predictions.

In an effort to validate the latest IRI 2012 model, a study was conducted by Chakraborty et al. (2014) based on TEC (Total Electronic Content) using Global Positioning System (GPS) satellites at four stations located between the equator and mid-latitudes: Port Blair (11.63°N, 92.70°E), Agartala (23.75°N, 91.25°E), Lhasa (29.65°N, 91.10°E), and Urumqi (43.46°N, 87.16°E) over

the course of a year. The study demonstrated reasonable agreement between the model and observed values in mid-latitude regions. However, a notable discrepancy between the TEC derived from IRI 2012 and ground observations in low-latitude regions was observed. The work also highlighted that this discrepancy appears to be more significant in low-latitude regions compared to mid-latitude regions.

The research conducted by Erdinç et al. (2021) aimed to improve the performance of the IRI-2016 model in forecasting foF2 across three latitudes in different hemispheres using data from six ionosonde stations: Manila (14.7°N, 121.1°E), Yamagawa (31.2°N, 130.6°E), Yakutsk (62.0°N, 129.6°E), Townsville (19.6°S, 146.8°E), Hobart (42.9°S, 147.3°E), and Terre Adelie (66.6°S, 140.0°E) during periods of both low and high solar activity. Their study concludes that the performance of the IRI-2016 model is strongly influenced by solar activity, latitude, seasonal altitude, local time, and hemisphere. In the northern hemisphere, relative deviations are most pronounced at high latitudes and least at mid-latitudes during both low and high solar activity. In the southern hemisphere, relative deviations are most significant at mid-latitudes during low solar activity and at low latitudes during high solar activity, with lower deviations at high latitudes.

Considering the findings from previous studies, it becomes necessary to investigate the diurnal variation of foF2 during disturbed geomagnetic periods with predictions from the IRI model at the Dakar station, which is situated near the Equatorial Ionization Anomaly (EIA). It has been noted that the URSI model provides better predictions for all phases of the solar cycle, with values approaching experimental measurements compared to CCIR in the African equatorial sector (Segda et al., 2019; Sawadogo et al., 2019). The objective of this article is to assess the predictability of the IRI 2016 model on days with varying durations of geomagnetic shocks (one-day shock, two-day shock, and three-day shocks) using data from the Dakar station during all phases of solar cycles 21 and 22.

MATERIALS AND METHODS

Data

The critical frequency of the F2 layer values measured at the Dakar station (latitude: 14.8°N; longitude: 342.6°E) were utilized. This station is situated in the northern ascending phase of the F2 region's ionization profile within a low-latitude zone. Operating from 1950 to 1993 for four solar cycles (cycles 19, 20, 21 and 22), the Dakar station's foF2 values were sourced from Télécom Bretagne (ENST-Bretagne). The foF2 values of the IRI model were obtained using the following website: http://omniweb.gsfc.nasa.gov. Aa geomagnetic index data and the dates of Sudden Storm Commencements (SSCs) were employed (Mayaud, 1973) to create a diagram. This diagram illustrates the variation of the geomagnetic index Aa as a function of solar activity for each rotation of the Sun, known as a Bartels rotation (Ouattara et al., 2009).

The geomagnetic index is derived from the K index measured at two antipodal mid-latitude stations. It quantifies the amplitude of global geomagnetic activity during 3 h intervals, normalized to geomagnetic latitude within ±50°. Mayaud (1971) introduced this index to monitor geomagnetic activity over an extended period. The daily average of the 8 tri-hourly values per day is denoted as Aa. An SSC corresponds to a sudden change in the geomagnetic field followed by a geomagnetic storm lasting less than 1 h. The dates of SSCs and the values of the Aa index since 1869 can be found on the ISGI website (http://isgi.unistra.fr). The mean annual sunspot number (Rz) was used to divide the solar cycles into phases. Rz values are available on the OMNIWEB website: https://omniweb.gsfc.nasa.gov/form/dx1.html.

Methods for classifying geomagnetic activity

Legrand and Simon (1989) and Richardson et al. (2000, 2002) carried out the first classification of days of geomagnetic activity using the pixel diagram. According to this classification, geomagnetic activity can be divided into four classes: Quiet activity which is associated with slow solar winds (V< 450 km/s); recurrent activity caused by fast solar winds from coronal holes (V> 450 km/s); shock activity which is related to shock waves due to CMEs; and fluctuating activity caused by fluctuations in the Sun's neutral plate. Ouattara and Amory-Mazaudier (2009) continued by developing criteria for selecting days of activity using the pixel diagram.

Days of geomagnetic activity are selected using the pixel diagram (Figure 1) proposed by Simon and Legrand (1989) and improved by Ouattara and Amory-Mazaudier (2009), who organized it into columns and rows; then, they defined a color code to make it easier to identify the different types of geomagnetic activity. A line in the pixel diagram corresponds to the period of one solar rotation (27 days). The SSC dates are represented by circles surrounding the value of the Aa index corresponding to the SSC day. The dates on which the Bartels cycle begins, the legend and the year are shown on the left, right and top of the pixel diagram respectively. According to the color code of the pixel diagram, the days of geomagnetic activity are selected as follows:

1. Quiets activities (QA) corresponding to index days aa ≤ 20 nT which are represented by white and blue boxes;
2. Recurrent activities (RA) corresponding to days when aa ≥ 40 nT and extending over one or more Bartels rotations without SSC; these days are represented by orange, red and bright red boxes over at least two successive days without SSC and over at least two solar rotations;
3. Shock activity (SA) corresponding to SSC days where aa ≥ 40 nT; these days are represented by a set of 1, 2 or 3 days represented by orange, red and/or olive red boxes with SSC at the start of the phase and without recurrence of SSC during 1, 2, 3 or 4 Bartels rotations;
4. Fluctuating activity (FA) which includes all the days not included in the three previous classes.

This study specifically examines the accuracy of foF2 predictions made by the IRI-2016 model during periods of shock activities (SAs). These SAs, which result from coronal mass ejections, are categorized into three types: One-day shocks, two-day shocks and three-day shocks. To better understand the influence of SAs, the research will analyze them separately for each duration. The pixel diagram can be used to identify these three types of SA (Aristide et al., 2018; Ali et al., 2022).

Criteria for dividing the solar cycle into phases

The solar cycle is divided into phases according to the criteria

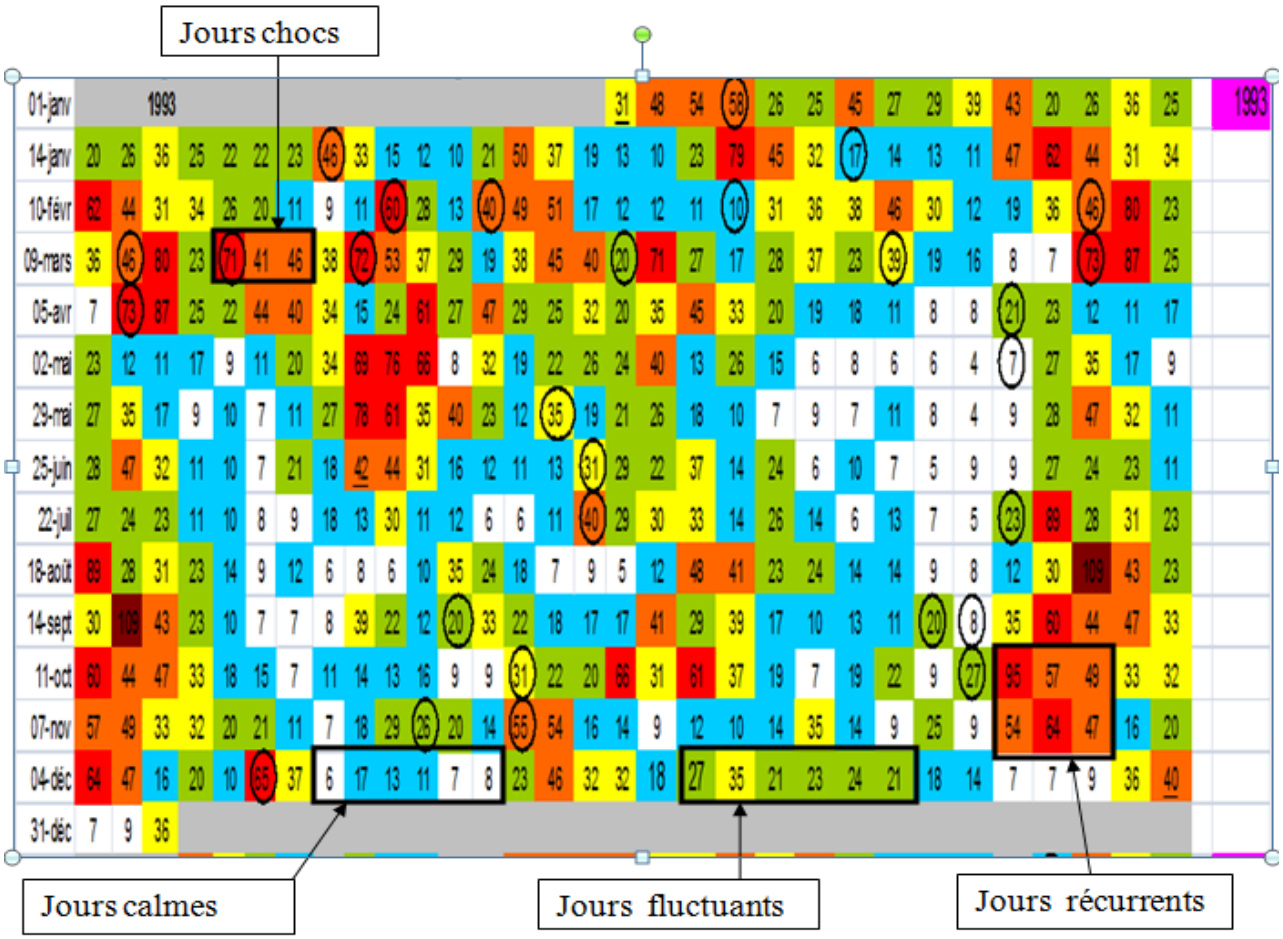

Figure 1. Pixel diagram of year 1993 using to determine geomagnetic activity classes.
Source: Ali (2016).

proposed by Gnabahou et al. (2013). These criteria take into account the mean annual sunspot number as: Minimum phase: Rz < 20; ascending phase: 20 ≤ Rz ≤ 100 with Rz greater than that of the previous year; maximum phase: Rz > 100 noting that for weak solar cycles (with Rz max <100) years of maximum phase correspond to those with an index Rz > 0.8 Rz max; and descending phase: 100 ≥ Rz ≥ 20 with Rz less than that of the previous year.

Data analysis methodology

In the African equatorial region, different types of profiles have been identified through studies on the diurnal variation of foF2. Five types of foF2 profile were determined by Faynot and Vila (1979): a "noon bite out" profile characterised by a double peak in the morning and evening with a trough around 12h00; the "morning peak" profile; the "inverse" profile; the "plateau" profile; and the "dome" type profile. These different profiles characterise the presence or absence of the electrojet or counter-electrojet (Fayot and Vila, 1979). The "noon bite out" profile indicates the presence of a strong electrojet; the "morning peak" profile indicates the presence of a medium electrojet; the "reversed" profile indicates the presence of a strong counter electrojet; the "plateau" and "dome" profiles indicate the total absence of these currents.

The percentage deviation is obtained using Equation 1:

$$\delta foF2 = \frac{foF2\ exp - foF2\ model}{foF2\ exp} * 100 \quad (1)$$

where foF2exp expresses the Dakar experimental data and the foF2 model designates the IRI Model data.

RESULTS

Figures 2 to 5 show the profiles of diurnal variations in foF2 during the SA of the experimental data and that of the URSI subroutine of the IRI-2016 model (left-hand column) and the curves of the relative percentage deviation of the model (right-hand column) during the minimum, ascending, maximum and descending solar phases respectively. Panels a, b and c refer to the one-day, two-day and three-day shocks respectively. The solid lines represent the experimental foF2 data from Dakar and the dashed lines represent the foF2 values from the IRI 2016 model.

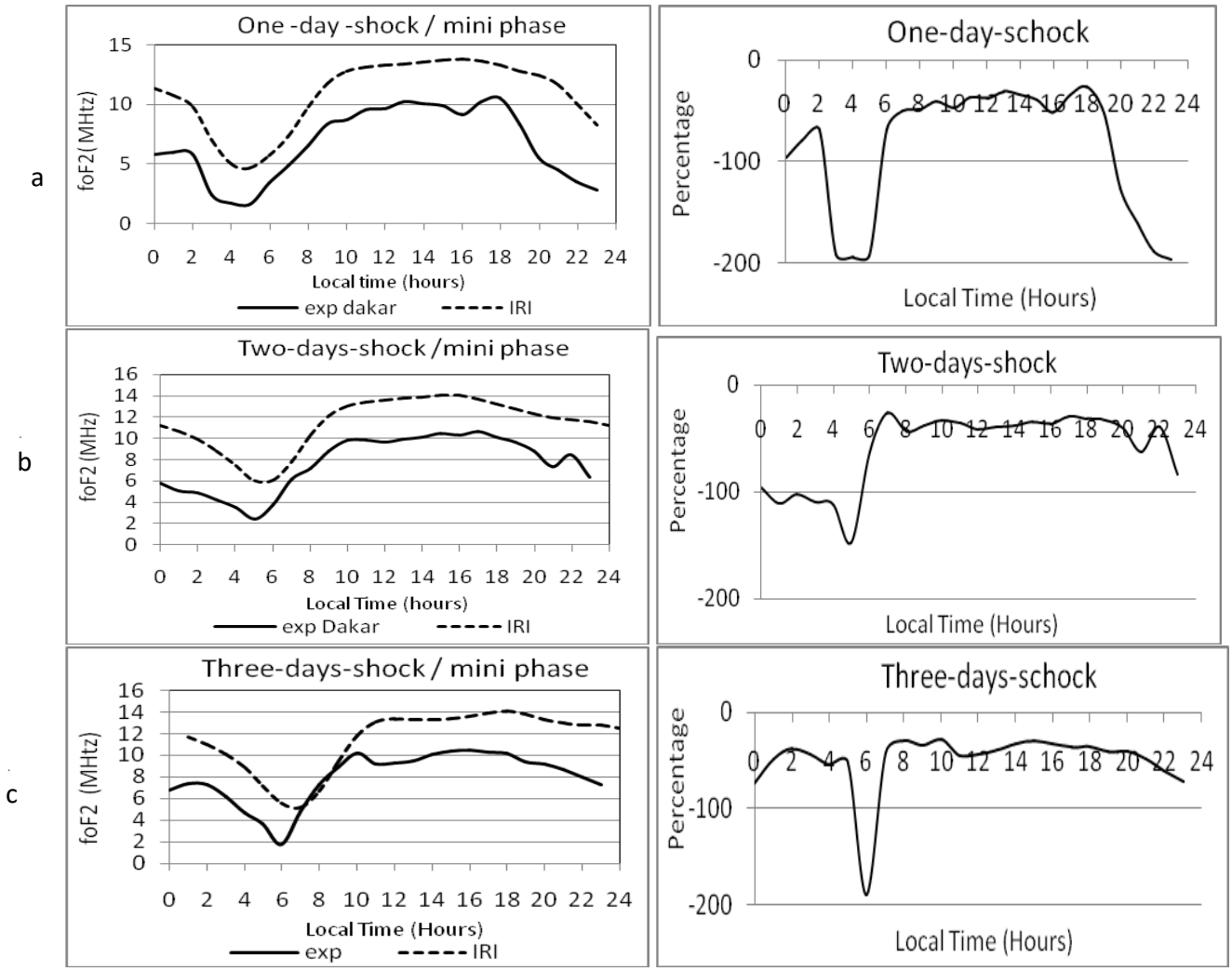

Figure 2. Profiles of diurnal variations in foF2 during the SA of the experimental data and that of the URSI sub-programme of the IRI-2016 model (left column) and curve of the relative percentage deviation of the model (right column) for the minimum phase.

Quality of foF2 prediction during SA at the Dakar station for the solar minimum phase

Figure 2a shows the one-day-shock during the solar minimum. The graphs from the IRI model show a plateau profile, whereas the curves from the experimental data show a “noon bit out” profile with a morning peak located at 13h00 (10.25 MHz) and an afternoon peak at 18h00 with a foF2 value of 10.50 MHz. The trough in this profile is around 16h00.The highest deviation percentages are recorded in the 03h00 to 06h00 time interval and are all negative.

The two-days-shock is marked by the total absence of electrojet because both graphs show a single type of profile, namely the plateau profile. In addition, the experimental foF2 data from Dakar show a night-time peak at 22h00 with a foF2 value of 8.45 MHz. The highest percentage was recorded at 05h00. During the three-days-shock, throughout the daytime, the graphs from the IRI model and those from the experimental data show almost similar daily variability in foF2.

The graph of the experimental data showed a noon bit out profile with a localized trough around 11h00; whereas the IRI model data showed a curve tending towards a plateau profile. The highest percentage was recorded at 06h00.

At solar minimum, the graphs of the experimental data globally show the signature of vertical drift, whereas the IRI model gives us a plateau profile characterizing the absence of electrojet.

Quality of foF2 prediction during SA at the Dakar station for the solar ascending phase

Figure 3 shows the diurnal variation in foF2 during the

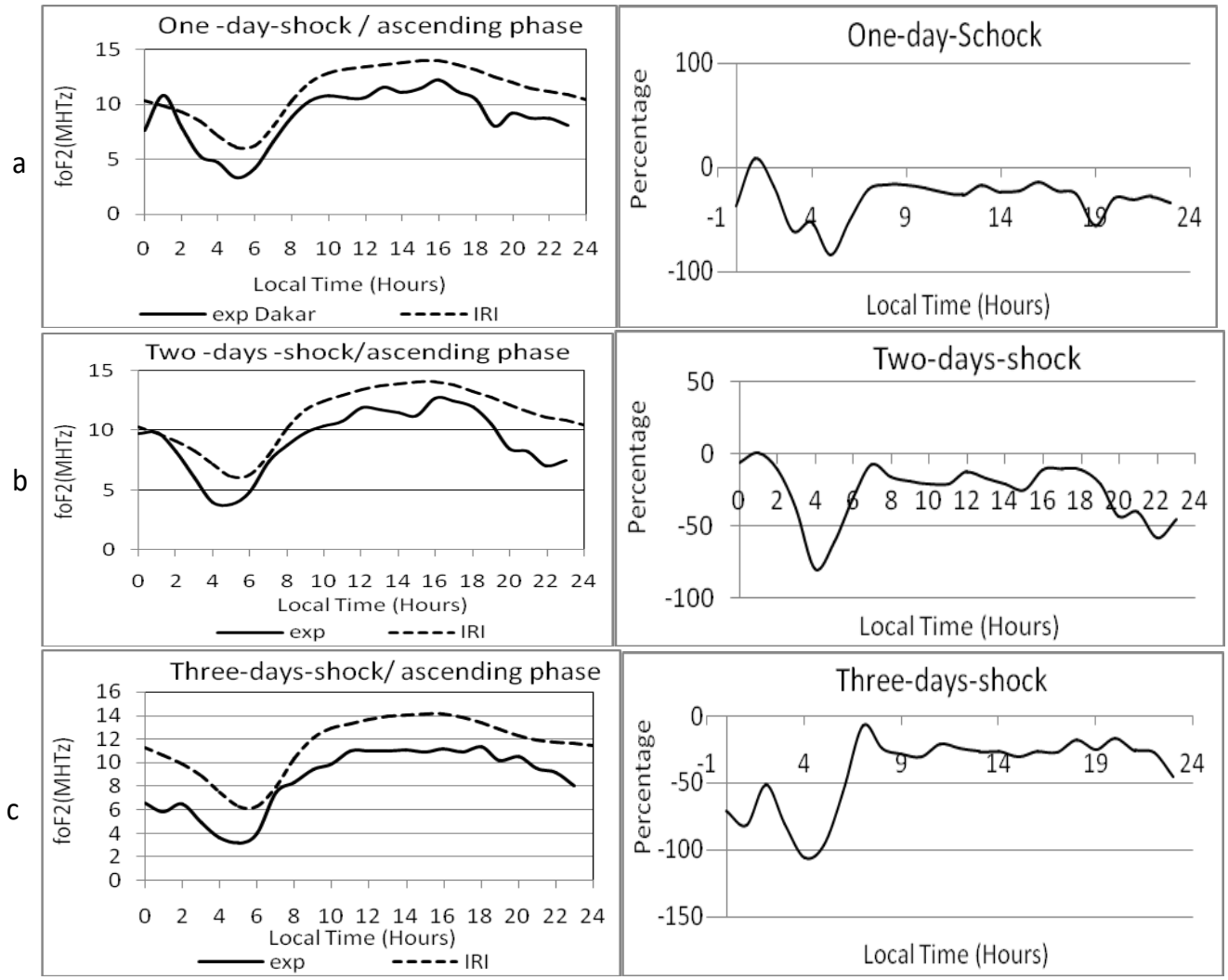

Figure 3. Profiles of diurnal variations in foF2 during the SA of the experimental data and that of the URSI sub-programme of the IRI-2016 model (left column) and curve of the relative percentage deviation of the model (right column) in the ascending phase.

increasing phase. During this phase, Panels q and b, which deal with the one-day-shock and two-days-shock respectively, clearly show the absence of electrojet in the IRI data, although the experimental data from Dakar show a disturbed noon bit out profile. During the one-day-shock, we note a positive value for the percentage deviation. This value is recorded at 01h00 with a percentage of 8.3%. The highest value for the percentage is always around sunrise (05h00).

During the two-days-shock, the highest percentage is observed at 04h00 (-79%). The three-days- shock is marked by the absence of electrojet observed on both graphs. With the exception of the three-days-shock, experimental data express the vertical drif ExB. As for the IRI model, the curves across the data always showed a plateau profile, which indicates the absence of this drift during this phase. The highest percentage was at 04h00. Considering the experimental data, the increasing phase is characterized at the Dakar station by a pre-reversal of the electric field on the different days of the shock.

Quality of foF2 prediction during SA at the Dakar station for solar maximum phase

At solar maximum, using the Panel a in Figure 4, which corresponds to the one-day-shock, we can see that experimental data show a slightly disturbed noon bit out profile with two small dips at 12h00 and 15h00; however, the graph of the IRI model shows a Dome profile. The highest percentage is noted at 01h00 with a positive value of 30%. During the two-days-shock and three-days-shock, experimental data show similar variation curves characterizing a counter-electrojet tending to disappear;

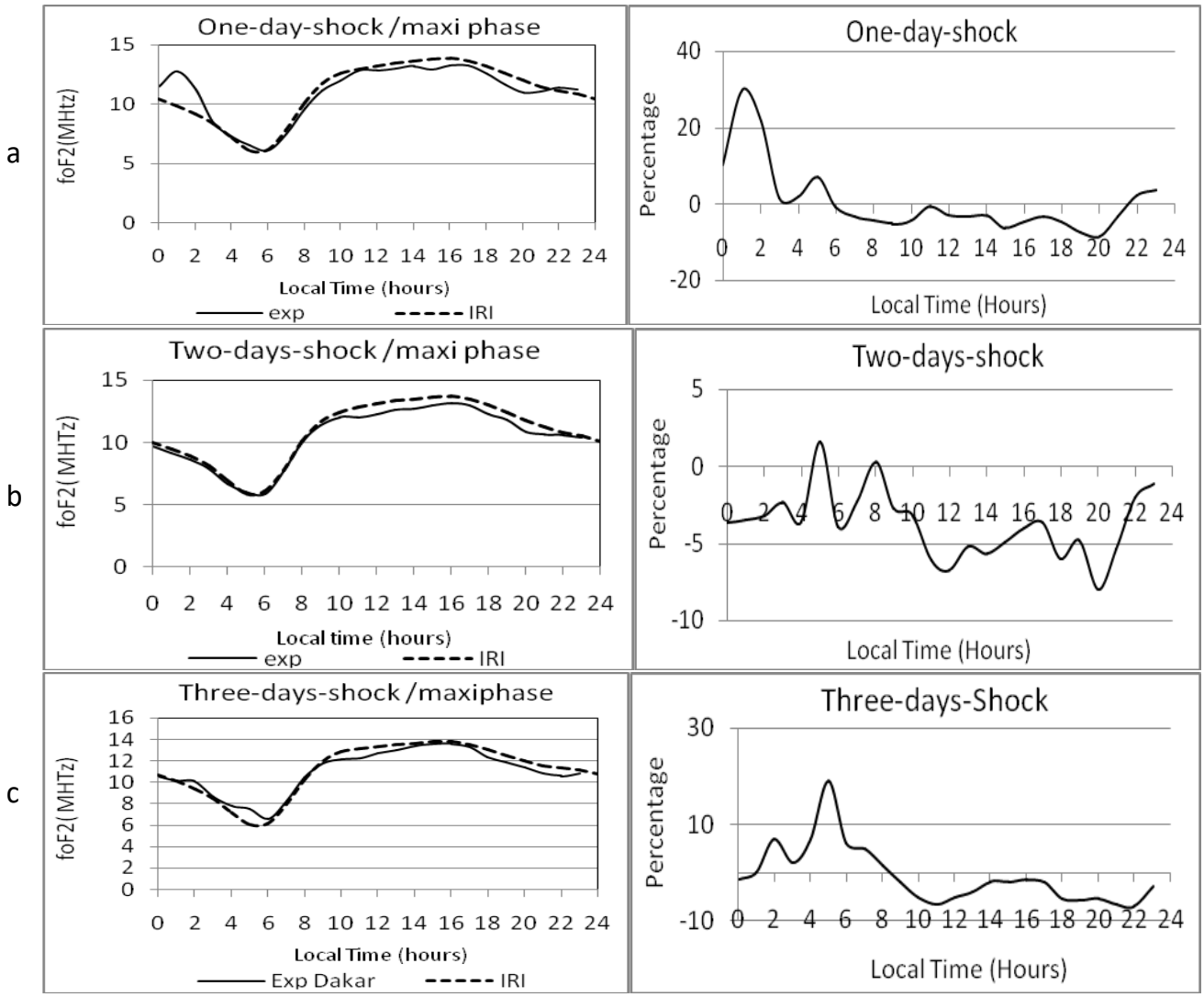

Figure 4. Profiles of diurnal variations in foF2 during the SA of the experimental data and that of the URSI sub-programme of the IRI-2016 model (left column) and curve of the relative percentage deviation of the model (right column) at the maximum phase.

however, through IRI, we record a plateau profile during the three-days-shocks and an absence of electrojet during the two-days-shock. At solar maximum, under the two-days-shock, we recorded percentage deviation values of less than 10%. During the three-days-shock, the highest percentage recorded was at 05h00 with a value of 19%. During this phase, the quantitative study showed a good correlation between the experimental data and the IRI model.

Quality of foF2 prediction during SA at the Dakar station for the solar descending phase

Figure 5a is devoted to one-day-shock during the decreasing phase. The plateau profile is observed on the curves of the IRI model and those of the experimental data. The maximum peak is observed at 16h00 with a value of 13.74 MHz for the IRI model, whereas the experimental data show this maximum at 17h00 with a foF2 value of 11.53 MHz

During the two-days-shock and three-days-shock, from the different curves obtained, we can say that the plateau profile is observed on the IRI model at the same time as the curves from the experimental data show the dome profile tending towards the plateau profile. In addition, experimental data from the one-day-shock show a night-time peak at 22h00 (9 MHz). During this phase, the highest values of percentage deviation were recorded at 00h00 during the one-day-shock and at 04h00 during the two-days-shock, with values equal to -81.69 and -77.19% respectively. The study concludes that the decreasing

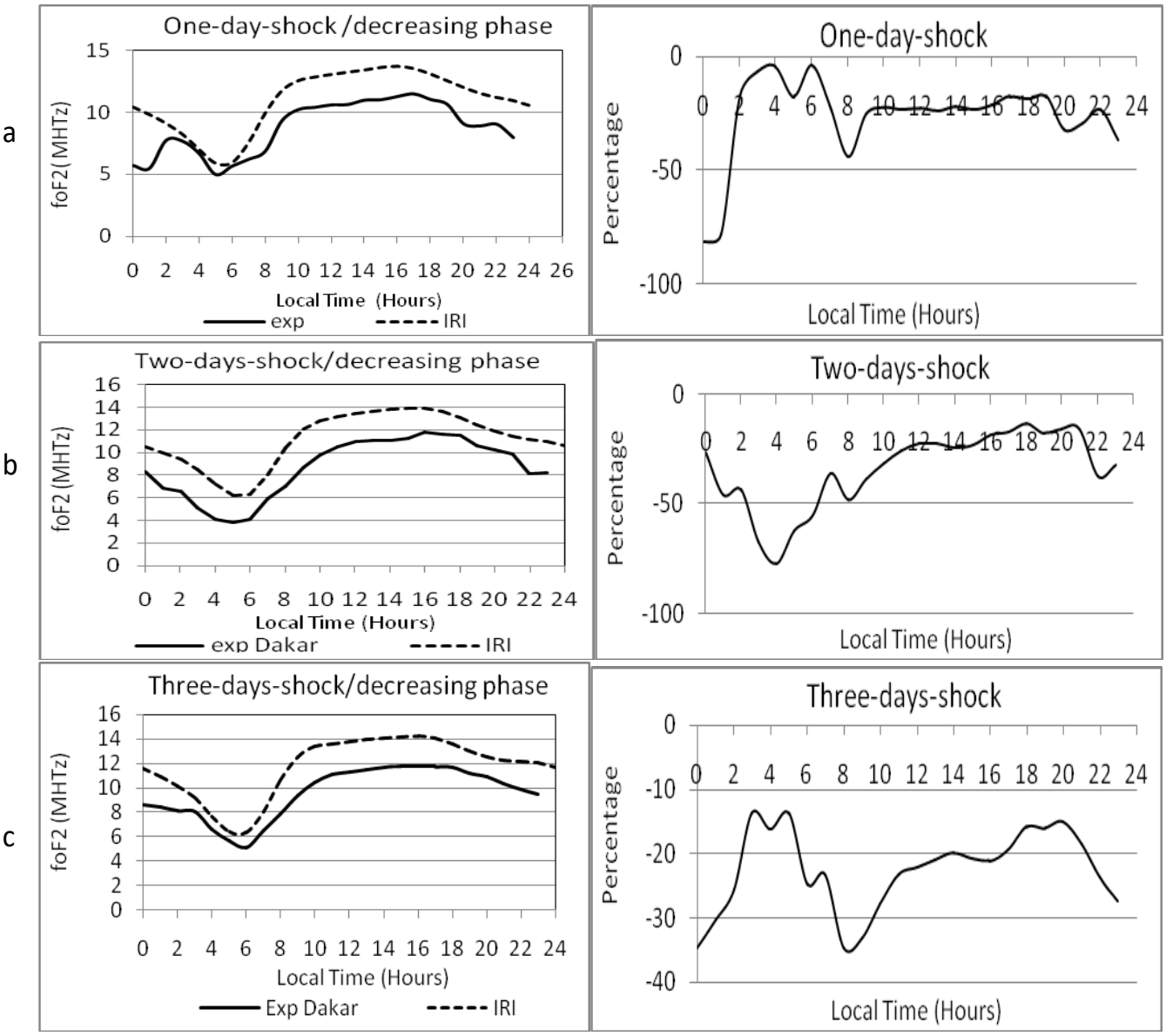

Figure 5. Profiles of diurnal variations in foF2 during SA of the experimental data and that of the URSI subroutine of the IRI-2016 model (left column) and curve of the percentage relative deviation of the model (right column) in the descending phase.

phase is marked by the total absence of electrojet.

DISCUSSION

The morphological study of the diurnal variation of foF2 made at the Dakar station during solar cycle 21 and 22 under the period of geomagnetic shock activity during different phases of the solar cycle shows that at solar minimum, experimental data show the ExB vertical drift signature, whereas the IRI model does not show this signature when it appears. This result corroborates the work carried out by Ouattara (2013) during the geomagnetic quiet activity at the Ouagadougou station from the period of 1985 to 1995 using the 2007 version (IRI) model, and that of Sandwidi et al. (2020) at the Dakar station during the same geomagnetic period but under two solar cycle (21 and 22).

Experimental data show a night-time peak indicating the signature of a pre-reversal of the electric field in the equatorial region during the increasing phase, but the IRI model does not show this signature. The same result was reported by Sawadogo et al. (2019) and Segda et al. (2019), during their studies at the Ougadougou station. The quantitative study through the percentage of deviation shows that the prediction is good during the day

compared to night. This result was found by Sandwidi et al. (2020) in their study at the same Dakar station but during the geomagnetic quiet activity using the same IRI 2016 model and was also shown by Guibula et al. (2019) using the Korogho station with the IRI 2012 model. Batista and Abdu (2004) also found good agreement between observed data and the model during the day.

Outside the maximum phase, IRI underestimates the observed data (the values of the IRI model are higher than those of the observed data). This result confirms the work carried out by Bertouni et al. (2006) using the Brazilian low-latitude station of Palmas (10.17°S, 48.20°W). At solar minimum, during one-day-shock, two-days-shock and three-days-shock, the averages of foF2 over the actual difference between the predicted and observed values are 3.9, 3.76 and 3.44 MHz, respectively. In increasing phase, these values are in the following order: 2.2, 2 and 2.8 MHz. In decreasing phase, these values are 2.14, 2.5 and 2.1 MHz.

The predictions were good during solar maximum. This result was also found by Batista and Abdu (2004) in their work on the comparative study between observed and IRI model ionospheric parameters at the Brazilian equatorial station of Sao Luis (2.6° S, 44.2°W, dip - 0.5°). In addition, it is important to note that the model shows high values of percentage deviation during the solar minimum on the different shock days. Very high values were also obtained by Guibula et al. (2019) using the Korogho station but with the IRI 2012 model.

Conclusion

This work deals with the study of the diurnal variation of foF2 carried out at the Dakar station during the geomagnetic shock period of variable duration during solar cycle 21 to 22 and its prediction with the IRI 2016 model. The analysis of the work shows that, whatever the solar phase, data of IRI model exhibit plateau or dome profiles types characterizing the absence of electrojet. The quantitative comparative study shows a good correlation between the data and the model during the maximum phase, while the opposite is true during the solar minimum. It should also be noted that the predictions are good during the daytime. Poor predictions are obtained overall at night. Except for the maximum phase, the study also shows that the model's foF2 values are higher than those of the experimental data. To improve the model, electrodynamics phenomena in the equatorial regions need to be taken into account.

CONFLICT OF INTERESTS

The authors have not declared any conflict of interests.

REFERENCES

Adeniyi JO, Oladipo OA, Radicella SM (2005). Variability of foF2 and comparison with IRI Model for an equatorial station. The Abdus Salam International Centre for Theoretical Physics 85:1-15.

Adewale AO, Oyeyemi EO, Ofuase UD (2010). Comparison between observed ionospheric foF2 and IRI-2001 predictions over periods of severe geomagnetic activities at Grahamstown, South Africa. Advances in Space Research 45:368-373.

Ali MN (2016). Statistical study of the critical frequency of the F2 layer in the Dakar and Ouagadougou stations:Comparison of the statistical data for solar cycle 21-22. Thesis supported at the University of Ouaga I Joseph Ki-zerbo (Burkina Faso).

Ali MN, Ouattara F, Anamo AT (2022). Comparative study of foF2 diurnal variation between the Dakar and Ouagadougou stations during the one-day, two-days and three-days shock periods for the solar minimum and maximum of cycle 21-22. Asian Journal of Sciences and Technology 13(09):12190-12192.

Aristide MFG, Doua AG, Ouattara F (2018). The Geomagnetic Effects of Solar Activity as Measured at Ouagadougou Station. International Journal of Astronomy and Astrophysics 8:178-190.

Batista IS, Abdu MA (2004). Ionospheric variability at Brazilian low and equatorial latitudes: comparison between observations and IRI model. Advances in Space Research 34:1894-1900.

Batista, IS, Abdu MA, de Medeiros RT, de Paula ER (1996). Comparison between IRI predictions and digisonde measurements at low latitude station. Advances in Space Research 18:49–52.

Bertoni F, Sahai Y, Lima WLC, Fagundes PR, Pillat VG, Becker-Guedes F, Abalde JR (2006). IRI-2001 model predictions compared with ionospheric data observed at Brazilian low latitude stations. Annales Geophysicae 24 :2191-2200.

Bittencourt, JA, Chryssafidis M (1994). On the IRI model predictions for the low-latitude ionosphere. Journal of Atmospheric and Terrestrial Physics 56:995-1009.

Chakraborty M, Kumar S, De BK, Guha A (2014). Latitudinal characteristics of GPS derived ionospheric TEC: a comparative study with IRI 2012 model.

Erdinç T , Hüseyin T , Samed İ , Munawar S , Punyawi J (2021). Assessment of improvement of the IRI model for foF2 variability over three latitudes in different hemispheres during low and high solar activities. Acta Astronautica 180:305-316.

Faynot JM, Vila P (1979). F region strata at the Magnetic Equator. Annales Geophysicae 35:1-9.

Gnabahou DA, Ouattara F, Nanéma E, Zougmoré F (2013). foF2 Diurnal Variability at African Equatorial Stations: Dip Equator Secular Displacement Effect. International Journal of Geosciences 4:1145-1150.

Guibula K, Zerbo JL, Kaboré M, Ouattara F (2019). Critical Frequency foF2 Variations at Korhogo Station from 1992 to 2001 Prediction with IRI-2012. International Journal of Geophysics, pp. 1-11.

Kumar S, Tan EL, Razul SG, See CMS, Siingh D (2014). Validation of the IRI-2012 model with GPS-based ground observation over a low latitude Singapore station. Earth Planets Space 66:17.

Legrand JP, Simon PA (1989). Solar cycle and geomagnetic activity: A review for geophysicists. Part I. The contribution to geomagnetic activity of shock waves and of the solar wind. Annales geophysicae 7(6).

Liu L, Wan W, Ning B, Zhang ML, He M, Yue X (2010). Longitudinal behaviors of the IRI-B parameters of the equatorial electron density profiles retrieved from FORMOSAT-3/COSMIC radio occultation measurements. Advances in Space Research 46:1064-1069.

Mayaud PN (1971). A planetary measurement of magnetic activity based on two antipodean observatories. Annales Geophysicae 27:67-70.

Mayaud PN (1973). A hundred-year series of geomagnetic data, 1868-1967: indices aa, storm sudden commencements. IAGA Bulletin 33:256.

Nanéma E, Ouattara F (2013). HmF2 quiet time variations at Ouagadougou and comparison with IRI-2012 and TIEGCM predictions during solar minimum and maximum. Archives of Applied Science Research 5:55-61.

Nanema E, Gnabahou DA, Zoundi C, Ouattara F (2018). Modeling the Ionosphere during Quiet Time Variation at Ouagadougou in West Africa. International Journal of Astronomy and Astrophysics 8:163.

Ouattara F, Amory-Mazaudier C (2009). Solar-geomagnetic activity and

Aa indices toward a standard classification. Journal of Atmospheric and Solar - Terrestrial Physics 71:1736-1748.
Ouattara F, Amory-Mazaudier C, Menvielle M, Simon P, Legrand JP (2009). On the long-term change in the geomagnetic activity during the 20th century. Annales Geophysicae 27(5):2045-2051.
Ouattara F (2013). IRI-2007 foF2 Predictions at Ouagadougou Station during Quiet Time Periods from 1985 to 1995. Archives of Physics Research 4:12-18.
Ouattara F, Nanéma E (2014). Quiet time foF2 variation at Ouagadougou station and comparison with TIEGCM and IRI-2012 prediction for 1985 and 1990. Physical Science International Journal 4:892-902.
Oyeyemi EO, Poole AW, Mckinell L (2005). On the global model for foF2 using neural networks. Radio science 40:1-15.
Richardson IG, Cliver EW, Cane HV (2000). Sources of geomagnetic activity over the solar cycle: relative importance of coronal mass ejections, high-speed streams, and slow solar 10 International Journal of Geophysics wind. Journal of Geophysical Research, Space Physics 105(A8):18203-18213.
Richardson IG, Cane HV, Cliver EW (2002). Sources of geomagnetic activity during nearly three solar cycles (1972– 2000). Journal of Geophysical Research: Space Physics 107(A8):SSH 8-1-SSH 8-13.
Sandwidi SA, Gnabahou DA, Ouattara F (2020). foF2 prediction with IRI 2016 at Dakar station during quiet activity over solar cycles 21 and 22. International Journal of Physical Sciences 15(4):194-200.
Sawadogo EW, Zerbo JL, Ali MN, Ouattara F (2019). Diurnal variation of F2-layer critical frequency under solar activity recurrent conditions during solar cycles 21 and 22 at Ouagadougou Station: Prediction with IRI-2012. Scientific Research and Essays 14(11):111-118.
Segda AK, Gnabahou DA, Ouattara F (2019). One-day-Shock, Two-days-Shock and Three-days-Shock foF2 diurnal variation with Solar cycle phases at Ouagadougou Station from 1966 to 1998: Comparison with IRI 2012 Predictions. Applied Physics Research 12(1):38-44.
Sethi NK, Dabas RS, Das RM (2007). Diurnal and seasonal variation of B0, B1 parameters during high solar activity period at low mid-latitude and their comparisons with IRI-2001 model. Journal of Atmospheric and Solar-Terrestrial Physics 69:767-774.
Shastri S, Aggarwal S, Sethi NK (1996). Performance of IRI model predictions of F-region for Indian latitudes. Advances in Space Research 18:41-44.
Simon PA, Legrand JP (1989). Solar cycle and geomagnetic activity: A review for geophysicists. Part II. The solar sources of geomagnetic activity and their links with sunspot cycle activity. Annales Geophysicae 7(6) 579-594.
Zhang Y, Paxton LJ, Bilitza D, Doe R (2010). Near real-time assimilation in IRI of auroral peak E-region density and equatorward boundary. Advances in Space Research 46:1055-1063.